Original Paper

Audiology & Neurotology

Audiol Neurotol 2007;12:209–220
DOI: 10.1159/000101328

Received: July 14, 2006
Accepted after revision: December 22, 2006
Published online: March 27, 2007

NF-kappaB-Dependent Apoptotic Hair Cell Death in the Auditory System

Ivana Nagy Antje Caelers Arianne Monge Sharouz Bonabi
Alexander M. Huber Daniel Bodmer

Inner Ear Research, Clinic for Otolaryngology, Head and Neck Surgery, University Hospital Zurich, NORD 2, and Center for Integrative Human Physiology (ZIHP), Zurich, Switzerland

Key Words
Apoptosis · Inner ear · Microarray · NF-kappaB inhibition · Phosphatidylinositol 3-kinase

Abstract
Hair cells are the most vulnerable elements in the inner ear and their degeneration is the most common cause of hearing loss. In the last few years progress has been made in uncovering the molecular mechanisms involved in hair cell damage and death. However, little is known about factors important for hair cell survival. Recently, it has been demonstrated that the transcription factor NF-kappaB is required for survival of immature auditory hair cells in vitro. Here we used DNA microarray technology to explore NF-kappaB downstream events in organ of Corti explants of postnatal day-5 Sprague-Dawley rats which were exposed to a cell-permeable NF-kappaB-inhibitory peptide. Gene expression was analyzed using DNA microarray technology. Genes were selected on the basis of comparative analysis, which reliably distinguished the NF-kappaB inhibitor-treated samples from control samples. Interestingly, among the up-regulated genes was the gene coding for the regulatory subunit of phosphatidylinositol 3-kinase. Moreover, inhibition of the phosphatidylinositol 3-kinase signaling pathway in organ of Corti explants exposed to the NF-kappaB inhibitor reduced caspase-3 activation. These data link NF-kappaB-dependent hair cell death to phosphatidylinositol 3-kinase signaling.

1. Introduction

Accurate statistics about hearing loss are not easy to obtain, however it is estimated that close to 250 million people worldwide suffer from some form of hearing impairment (http://www.who.org). One in every 1000 children are deaf by the age of 3 as a result of a number of inherited conditions, premature birth or complications during birth [Nadol, 1993]. In adults, hearing loss is often gradual and for many people begins around age 55, or it can be sudden, resulting from injury or infection. Other common causes of hearing impairment include exposure to intense sound (i.e. noise-induced hearing loss) and treatment with damaging medication (e.g. aminoglycoside antibiotics, anticancer drugs such as carboplatin and cisplatin, some loop diuretics and malaria medicine) [Huang et al., 2000; Johnsson et al., 1981; Yorgason et al., 2006]. In most cases of hearing loss, the cause is linked to degeneration and death of cochlear sensory elements (i.e. hair cells). Since hair cells (HCs) in mammals do not re-

I.N. and A.C. contributed equally to this paper.

KARGER

Fax +41 61 306 12 34
E-Mail karger@karger.ch
www.karger.com

1420–3030/07/0124–0209$23.50/0

Accessible online at:
www.karger.com/aud

Daniel Bodmer
University Hospital Zurich, Clinic for Otolaryngology
Head and Neck Surgery, Frauenklinikstrasse 24
CH–8091 Zurich (Switzerland)
Tel. +41 44 255 1111 (163-220), Fax +41 44 255 4164, E-Mail daniel.bodmer@usz.ch

generate, this type of hearing loss is irreversible. A detailed understanding of the molecular events involved in HC damage and death is essential for developing prophylactic and therapeutic strategies to prevent hearing loss associated with HC damage and death.

Over the past few years considerable progress has been made in discovering factors that mediate HC death, however, little is known about factors important for HC survival. Recently, we could demonstrate that NF-kappaB, a transcription factor that plays a major role in the regulation of many apoptosis- and stress-related genes, is required for the survival of immature auditory HCs in vitro [Nagy et al., 2005]. In most cells, NF-kappaB is kept inactive in the cytoplasm through interaction with I-kappaB. Nuclear translocation occurs after stimulus-induced degradation of I-kappaB. In addition to the inducible form, a constitutive active NF-kappaB has been described in different cell types such as photoreceptor cells in the eye and cortical neurons [Kaltschmidt et al., 1994; Krishnamoorthy et al., 1999]. Similar to these reports we found a constitutively active form of NF-kappaB in the organ of Corti (OC) of 5-day-old rats. Selective inhibition of NF-kappaB in vitro caused massive degeneration of HCs within 24 h of inhibitor application [Nagy et al., 2005]. These data suggest an important role for NF-kappaB in mediating survival of immature auditory HCs. We initiated this study to explore NF-kappaB downstream events that contribute to HC survival in the immature mammalian cochlea.

2. Materials and Methods

2.1. Animal Procedures

All animal procedures were carried out according to protocols approved by the Kantonales Veterinäramt, Zurich, Switzerland. Postnatal day 5 (p5) Sprague-Dawley rats (Harlan, The Netherlands) were utilized throughout the study.

2.2. Organ Culture

Animals were sacrificed and the cochleae carefully dissected to separate the OC from the spiral ganglion, stria vascularis and Reissner's membrane. The organs were placed into 0.4-μm culture plate inserts (Millipore AG, Switzerland) and maintained in Dulbecco's modified Eagle medium, supplemented with 10% fetal calf serum, 25 mM HEPES and 30 U/ml penicillin (Invitrogen AG, Switzerland). In all experiments, an 8-hour period was allowed for the explants to recover from the isolation procedure before further treatments [Sobkowicz et al., 1993]. For the time-course experiment, explants were exposed for 6, 12, and 24 h, respectively, to the NF-kappaB inhibitor, while control explants were kept in culture medium alone or were exposed to the inactive control NF-kappaB inhibitor for 24 h (7 OC explants per sample). For the triplicate experiment, OC explants were exposed to the NF-kappaB inhibitor for 6 h, control explants were kept in culture medium alone or were exposed for 6 h to the inactive control NF-kappaB inhibitor (7 OC explants per sample). Each experiment was performed 3 times.

2.3. Inhibition of NF-kappaB Activity

To inhibit NF-kappaB activity, an HPLC-purified synthetic inhibitor (NF-kappaB inhibitor, AAVALLPAVLLALLAPVQRKRQKLMP, Santa Cruz Biotechnology Inc., Santa Cruz, Calif., USA) was added to the cell culture medium at the final concentration of 25 μg/ml. We have previously shown that this compound and concentration causes HC loss [Nagy et al., 2005]. In the control experiments, an inactive control for the NF-kappaB inhibitor was used (NF-kappaB control, AAVALLPAVLLALLAPVQRDGQKLMP, Santa Cruz Biotechnology Inc.) at the same final concentration.

2.4. Inhibition of Phosphatidylinositol 3-Kinase Activity

Liquid LY 294002 (Calbiochem, Merck Biosciences GmbH, Germany), a highly specific, cell-permeable phosphatidylinositol 3-kinase (PI3-K) inhibitor was added to the cell culture medium at the final concentration of 20 μM. OC explants were first pretreated with LY 294002 for 2 h. Following pretreatment, a medium change was performed and samples were treated either with the NF-kappaB inhibitor (as described above) and LY 294002 simultaneously, or only LY 294002, for 24 h.

2.5. RNA Extraction from the OC

Total RNA was prepared from the cultured OC explants. Immediately following treatment, tissue was placed in RNAlater (Qiagen AG, Switzerland) for a period of 2 days. Seven OC explants were pooled in one sample in order to obtain enough material for further study. RNA was prepared using the RNAeasy Mini Kit (Qiagen AG, Switzerland) according to manufacturer's instructions. DNase I treatment was performed directly on the columns, also following the supplied protocol. The quality of the isolated RNA was determined with a NanoDrop ND 1000 (NanoDrop Technologies, Delaware, Ohio, USA) and Bioanalyzer 2100 (Agilent, Waldbronn, Germany). Only those samples with a 260/280-nm ratio between 1.8 and 2.1 and a 28S/18S ratio within 1.5–2 were further processed.

2.6. Description of the Time-Course Microarray Experiments

2.6.1. cRNA Preparation. Total RNA (100 ng) was reverse-transcribed into double-stranded cDNA with the Two-Cycle cDNA Synthesis Kit (Affymetrix Inc., P/N 900494, Santa Clara, Calif., USA). The double-stranded cDNA was purified using a Sample Cleanup Module (Affymetrix Inc., P/N 900371). The purified double-stranded cDNA was in vitro transcribed in the presence of biotin-labeled nucleotides using a IVT Labeling Kit (Affymetrix Inc., P/N 900449). The biotinylated cRNA was purified using a Sample Cleanup Module (Affymetrix Inc., P/N 900371) and its quality and quantity were determined using NanoDrop ND 1000 and Bioanalyzer 2100.

2.6.2. Array Hybridization. Biotin-labeled cRNA samples (15 μg) were fragmented randomly to 35–200 bp at 94°C in Fragmentation Buffer (Affymetrix Inc., P/N 900371) and mixed in 300 μl of hybridization buffer containing a hybridization control cRNA and control Oligo B2 (Affymetrix Inc., P/N 900454), 0.1 mg/ml herring sperm DNA and 0.5 mg/ml acetylated bovine serum al-

bumin in 2-(4-morpholino)-ethane sulfonic acid buffer, pH 6.7, before hybridization to GeneChip® Rat Genome 230 2.0 arrays for 16 h at 45°C. Arrays were then washed using an Affymetrix Fluidics Station 450 EukGE-WS2v5_450 protocol. An Affymetrix GeneChip Scanner 3000 (Affymetrix Inc.) was used to measure the fluorescent intensity emitted by the labeled target.

2.6.3. Statistical Analysis. Raw data processing was performed using the Affymetrix GCOS 1.2 software (Affymetrix Inc.). After hybridization and scanning, probe cell intensities were calculated and summarized for the respective probe sets by means of the MAS5 algorithm [Hubbell et al., 2002]. To compare the expression values of the genes from chip to chip, global scaling was performed, which resulted in the normalization of the trimmed mean of each chip to a target intensity (TGT value) of 500 as detailed in the statistical algorithms description document of Affymetrix (2002). Quality control measures were considered before performing the statistical analysis. These included adequate scaling factors (between 1 and 3 for all samples) and appropriate numbers of present calls calculated by application of a signed-rank call algorithm [Liu et al., 2002]. The efficiency of the labeling reaction and the hybridization performance was controlled with the following parameters: present calls and optimal 3′/5′ hybridization ratios (around 1) for the housekeeping genes (GAPDH and ACO7), for the poly-A spike in controls and the prokaryotic control (BIOB, BIOC, CREX, BIODN).

2.7. Description of the Triplicate Microarray Experiment

2.7.1. cRNA Preparation. Preparation of cRNA was performed as described in section 2.6.1 with the difference that total RNA samples (2 μg) were reverse-transcribed into double-stranded cDNA with one-cycle cDNA synthesis kit (Affymetrix Inc., P/N 900431).

2.7.2. Array Hybridization. Array hybridization was performed as described in 2.6.2.

2.7.3. Statistical Analysis. Statistical analysis was performed as described in 2.6.3.

2.8. DNA Chip Analysis

Analysis of the microarray data was performed using DNA chip (dChip) software [Cheng and Wing, 2001], version June 27, 2005 (available at: http://www.dchip.org, a detailed description of model-based analysis of oligonucleotide arrays can be found at this website). Individual array intensities were normalized to the array with median overall intensity using the Invariant Set of Normalization method (per default). Model-based expression values were computed using the PM/MM difference model, measurement error was considered when averaging. In the main experiment, the following comparison criteria were used to assess differentially expressed genes between the baseline set (B = three Nt groups and three Mut_6h-treated groups) and the experiment set (E = three Inh_6h-treated groups): (i) lower 90% confidence bound of fold change; (ii) $E/B > 1.2$, $B/E > 1.2$; (iii) $E - B > 100$, $B - E > 100$; (iv) p value for testing $E = B \leq 0.05$, P call of $B \geq 20\%$, P call of $E \geq 20\%$. Filtering was applied to cutoff variation across samples after pooling of replicate assays to $0.5 <$ standard deviation/mean < 100, P call % in the arrays used $\geq 20\%$, and expression level ≥ 20 in $\geq 50\%$ samples. Finally, clustering was performed with setting the p value threshold for calling significant clusters between 0.001 and 0.05. The results are displayed in the form of a clustering tree.

2.9. GeneSpring Analysis

GeneSpring 7.1 software package (Agilent Technologies, Inc.) was used as an alternative microarray analysis tool to double-check data generated by dChip analysis. Affymetrix-generated.cel files were loaded into GeneSpring software. Preprocessing (i.e. chip background intensity adjustment) was performed using GC-Robust Multiarray Analysis (GC-RMA), per default. Data were normalized across all chips using the median of each gene. Only measurements flagged as present and with the raw signal value of 100 were filtered further using the cross-gene error model based on replicates (software supplier's instructions were followed as described in the analysis guide for cross-gene error model available at http://www.chem.agilent.com), p value cutoff was set at 0.05.

2.10. Real-Time PCR

TaqMan® Gene Expression Assays with probes Rn00580055_m1 [cysteine-rich protein 61 (Cyr61)], Rn00564547_m1 [regulatory subunit of PI3-K (PI3-Kr1)], Rn00594145_m1 [cadherin-13 (Cdh13)] and the endogenous controls Rn_00566655_m1 [beta-glucuronidase (Gusb)] and beta actin (4352931E) were used to verify changes in gene expression levels. Assays were performed in the ABI PRISM 7700 Sequence Detection System according to manufacturer's protocol (Applied Biosystems, Applera Europe B.V., The Netherlands). For each reaction, cDNA samples were diluted 1:10 and 1 μl was used together with the TaqMan® Universal PCR Master Mix., No AmpErase® UNG (Applied Biosystems, P/N 4234018, Applera Europe B.V., The Netherlands). After completion of 45 cycles at default settings, resulting amplification curves were examined and baseline values were set between cycles 3 and 15 (no adjustment was necessary), log increase was observed to start at cycle 22. Expression of each target mRNA was calculated using the comparative C_t method, based on the threshold cycle (C_t) as $2^{-c\Delta\Delta Ct}$, where $\Delta C_t = C_{t,\ \text{target}} - C_{t,\ \text{Gusb or beta-actin}}$ and $\Delta\Delta C_t = \Delta C_{t,\ \text{experiment condition}} - \Delta C_{t,\ \text{control condition}}$. Standard deviations (s) were calculated according to the formula $s = (s_{\text{control condition}}^2 + s_{\text{experiment condition}}^2)^{1/2}$.

2.11. Immunofluorescence

For immunofluorescence studies, OC explants were fixed in 4% paraformaldehyde in phosphate-buffered saline (PBS) (pH 7.2) and permeabilized with 5% Triton X-100 in PBS with 10% fetal bovine serum. To reduce unspecific binding sections were treated with PBS containing 2% bovine serum albumin for 30 min at room temperature. The samples were then incubated with rabbit anti-PI3-K p85α polyclonal antibody (Z-8) (1:50) overnight at 4°C. After repetitive washing in PBS, the samples were incubated with secondary anti-rabbit FITC-conjugated antibody (1:100) for 2 h at room temperature. In the negative control, the primary antibody was replaced by PBS. Samples were visualized on a fluorescence microscope (Olympus IX71) and photographed using AxioCam (Zeiss) immediately following staining. All antibodies were purchased from Santa Cruz Biotechnology Inc. (Santa Cruz, Calif., USA).

For phalloidin staining samples were incubated with a 1:100 dilution of F-actin binding Texas red-conjugated phalloidin T7471 (Invitrogen AG) for 1 h at room temperature. Visualization was performed on a Leica inverted confocal laser scanning microscope with a red filter (excitation/emission wavelength 596/615nm). Images were assembled by stacking 20 single digital scans (4 μm in thickness) using Imaris® Image Processing Software (Bitplane AG, Switzerland).

2.12. Caspase-3 Activity Assay

Cultured OC explants were harvested in 10 mM HEPES, pH 7.5, 2 mM EDTA and 0.1% CHAPS, supplemented with 5 mM DTT, 1 mM PMSF, 10 μg/ml pepstatin A, 10 μg/ml aprotinin and 10 μg/ml leupeptin. For each condition, 5 explants were pooled in order to obtain enough material for biochemical assays. Tissue was homogenized with Ultra-Turrax T8 (IKA-Werke GmbH, Germany) tissue homogenizer. Samples were then centrifuged at 13,000 rpm for 20 min at 4°C, and supernatant mixed 1:1 with caspase assay buffer (200 mM HEPES, pH 7.5, 1 mM EDTA, 20% sucrose, 0.2% CHAPS, 0.2 mg/ml bovine serum albumin, 20 mM DTT). Adenosine triphosphate (Invitrogen AG) and Ac-DEVD-pNA (ALEXIS Corp., Switzerland) were added to the reaction mixtures at the final concentrations of 1 and 50 mM, respectively. Reactions were incubated for 3 h at 37°C. Following, the caspase-3 activity was measured in a spectrophotometer (Tecan Trading AG, Switzerland) at wavelength 405 nm.

2.13. Statistical Analysis for Caspase Assays

Results obtained in the caspase activity assays were analyzed by an unpaired t test using GraphPad Prism 3.03 software (GraphPad Software Inc.). The unpaired t test compares the means of two groups, assuming the data are sampled from Gaussian populations. Statistical significance is given in the form of p value and confidence interval. A p value of <0.05 signifies that the differences observed in comparison of 2 samples are statistically significant, i.e. that it is unlikely that the differences observed are due to a coincidence of random sampling. Data obtained in three independent experiments were used for analysis.

3. Results

3.1. Inhibition of NF-kappaB Activity in OC Explants Results in Gene Expression Changes Compared to Control Explants

To assess the time point at which global changes in gene expression occur in rat p5-old OC explants exposed to 25 μg/ml NF-kappaB inhibitor, gene expression profiling was performed using GeneChip® Rat Genome 230 2.0 arrays from Affymetrix. In this experiment, out of 31099 sequence tags present on the gene chip, statistical analysis (p value between 0.001 and 0.05) identified 74 differentially expressed genes 6 h after addition of the NF-kappaB inhibitor compared to untreated samples or samples treated with the inactive NF-kappaB inhibitor control (fig. 1, down-regulated genes are depicted in blue, up-regulated genes are depicted in red). A list containing a more detailed description of differentially expressed genes, as identified by dChip software, is provided in table 1. It must be noted that these data represent a single array sample employing specific experimental conditions, and the genes presented in figure 1 are not to be regarded as reliably differentially expressed between the tested conditions. We used them as orientation for determining an early time-point at which NF-kappaB inhibition-induced gene expression changes could be observed in OC cultures.

3.2. After 6 h of NF-kappaB Inhibition, the OC Explants Do Not Show HC Loss

Previously, we have shown that caspase-3 activation in OC explants occurs as early as 6 h after treatment with the NF-kappaB inhibitor, with apoptotic HC death visible after 24 h [Nagy et al., 2005]. Here we extend the histological analysis to earlier points in time of 6 and 12 h, with an inhibitor concentration of 25 μg/ml throughout the experiments. Six hours of treatment did not result in any significant HC loss, although the HC rows appeared slightly perturbed (fig. 2). Twelve hours following treatment, visible damage to HC could be detected (fig. 2). A total of 8 explants (from 4 animals) were examined for each condition; representative images are shown in figure 2.

3.3. The Regulatory Subunit of PI3-K Is Up-Regulated in HCs after NF-kappaB Inhibition

After determining that gene expression changes occur as early as 6 h following NF-kappaB inhibition, this time was chosen for further analysis in which the microarray experiments were performed in triplicates, and the data analyzed by dChip and GeneSpring software packages. Both comparative analyses gave overlapping results and have identified 14 genes, which reliably distinguished the NF-kappaB inhibitor-treated samples from control samples either cultured in medium alone or treated with the inactive control NF-kappaB inhibitor (fig. 3). From 14 genes, 2 were down-regulated, and 12 were up-regulated following NF-kappaB inhibition (table 2).

Out of the 14 genes found in the replicate assays to be reliably differentially expressed in the NF-kappaB inhibitor-treated group vs. the inactive control inhibitor group and the medium alone control group, two genes were selected and their expression changes were then assessed using RT real-time PCR. The gene coding for PI3-Kr1 and the gene coding for Cyr61 were chosen for analysis because of previous reports linking NF-kappaB to these genes [D'Addario et al., 1999; Lin et al., 2004]. RT real-time PCR confirmed up-regulation of PI3-Kr1 and Cyr61 genes and down-regulation of the Cdh13 gene in NF-kappaB inhibitor-treated OC explants, as compared to untreated controls (fig. 4a–c). Moreover we could detect PI3-Kr1 in inner and outer HC of the OC. PI3-Kr1 immunoreactivity was only present in HCs and not in any type of supporting cells. After inhibition of NF-kappaB the immunoreactivity was significantly increased (fig. 5).

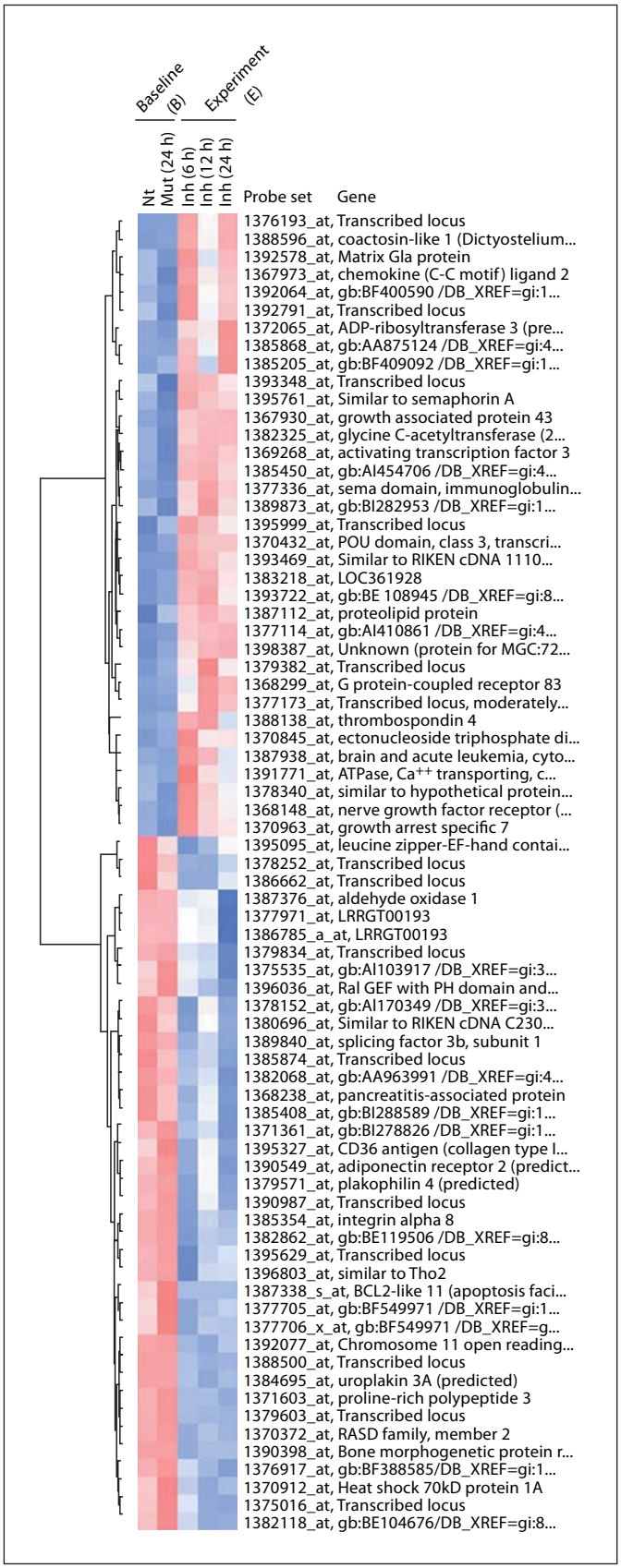

Fig. 1. dChip clustering tree representing the time-course experiment data. Differentially expressed genes in the OC explants following 6-, 12-, and 24-hour treatment with a specific NF-kappaB inhibitor (Inh), compared to untreated (Nt) and inactive inhibitor control (Mut)-exposed OC explants. Each row represents a gene, and each column represents a sample. The dendrogram on the left illustrates the results of clustering, where genes close to each other have high similarity in their standardized values across all samples. The expression level of each gene is standardized to have mean 0 and standard deviation 1. Red color represents expression levels above mean expression and blue color represents expression lower than mean.

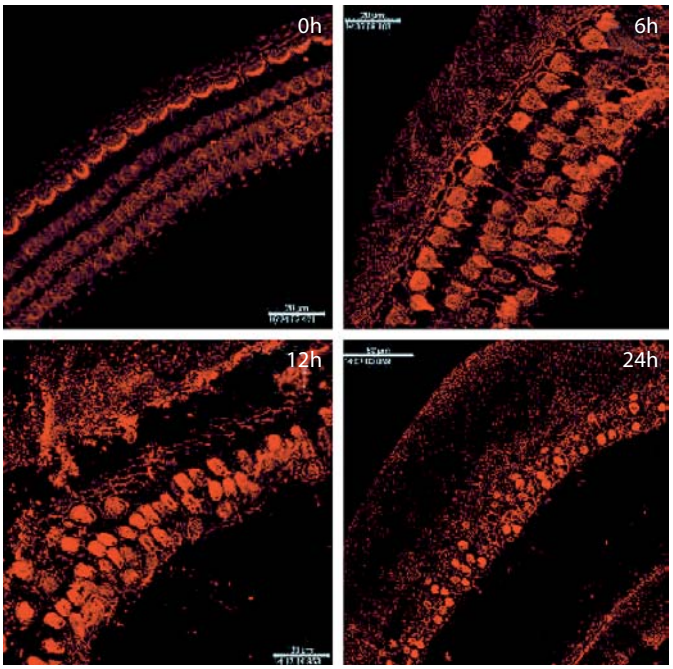

Fig. 2. NF-kappaB inhibitor damages HCs. Middle turns of rat p5 OC organs immunostained with phalloidin-rhodamine analyzed by immunofluorescence microscopy. Explants were treated with a specific NF-kappaB inhibitor for 0 (control, cultured in medium alone), 6, 12, and 24 h. There is progressive HC loss with increasing time of exposure to the inhibitor.

Table 1. Time-course microarray experiment data

	Gene symbol	Description	NCBI GeneID or locus	Fold change
1	EST		AA819658	+1.49
2	Cotl1_predicted	coactosin-like 1 (predicted)	361422	+1.44
3	Mgp	matrix Gla protein	5333	+1.9
4	Ccl2	chemokine (C-C motif) ligand 2	24770	+1.84
5	EST		BF400590	+1.74
6	EST		AA964492	+1.58
7	Art3_predicted	ADP-ribosyltransferase 3 (predicted)	305235	+1.43
8	EST		AA875124	+1.36
9	EST		BF409092	+2.54
10	EST		AI007775	+1.64
11	Sema3b_predicted	secreted, (semaphorin) 3B (predicted)	63142	+1.39
12	Gap43	growth-associated protein 43	29423	+1.82
13	Gcat_predicted	lycine C-acetyltransferase (predicted)	366959	+1.49
14	Atf3	activating transcription factor 3	25389	+1.65
15	EST		AI454706	+1.49
16	Sema3b_predicted	secreted, (semaphorin) 3B (predicted)	363142	+1.39
17	EST		BI282953	+1.49
18	EST		BF419607	+1.48
19	Pou3f1	POU domain, class 3, transcription factor 1	192110	+1.91
20	RGD1307901_ predicted	similar to RIKEN cDNA 1110001E1 (predicted)	306327	+1.43
21	LOC361928		361928	+1.37
22	EST		BE108945	+1.34
23	Plp	proteolipid protein	24943	+1.51
24	EST		AI410861	+1.4
25	RGD:735075	unknown (protein for MGC: 72614)	310540	+1.53
26	EST		AI144865	+1.6
27	Gpr83	G protein-coupled receptor 83	140595	+1.63
28	EST		BE104535	+1.39
29	Thbs4	thrombospondin 4	29220	+1.48
30	Entpd2	ectonucleoside triphosphate diphosphohydrolase 2	64467	+1.62
32	Baalc	brain and acute leukemia, cytoplasmic 1	140720	+1.63
33	Atp2a2	ATPase, Ca++ transporting slow twitch 2	29693	+1.72
34	LOC289480	similar to hypothetical protein MGC35043	89480	+2.06
35	Ngfr	nerve growth factor receptor (TNFR superfamily, member 16)	24596	+1.86
36	Gas7	growth arrest-specific 7	85246	+1.52
37	Letm2_predicted	leucine zipper-EF-hand containing transmembrane protein 2 (predicted)	361169	–2.21
38	EST		AI029745	–1.63
39	EST		BF553981	–5.14
40	Aox1	aldehyde oxidase 1	54349	–2.47
41	EST		BG378771	–1.84
42	EST		BF559982	–1.94
43	EST		BG374488	–2.82
44	EST		AI103917	–2.2
45	Ralgps2_predicted	Ral GEF with PH domain and SH3 binding motif 2 (predicted)	304887	–1.51
46	EST		AI170349	–1.63
47	RGD1310037_ predicted	similar to RIKEN cDNA C230093N12 (predicted)	365903	–2.74
48	Sf3b1	splicing factor 3b, subunit 1	84486	–1.33
49	EST		AA956418	–2.19
50	EST		AA963991	–1.48
51	Pap	pancreatitis-associated protein	24618	–1.43
52	EST		BI288589	–1.64
53	EST		BI278826	–1.42

Table 1 (continued)

	Gene symbol	Description	NCBI GeneID or locus	Fold change
54	Scarb2	CD36 antigen (collagen type I receptor, thrombospondin receptor)-like 2	117106	–1.75
55	Adipor2_predicted	adiponectin receptor 2 (predicted)	12670	–1.51
56	Pkp4_predicted	plakophilin 4 (predicted)	295625	–1.94
57	EST		AI406858	–1.81
58	Itga8	integrin alpha 8	84381	–1.57
59	EST		BE119506	–1.35
60	EST		BE105336	–1.49
61	LOC313308	similar to THO complex 2	313308	–1.6
62	Bcl2l11	BCL2-like 11 (apoptosis facilitator)	64547	–17.6
63	EST		BF549971	–1.56
64	C11orf8	chromosome 11 open reading frame 8	362185	–1.51
65	EST		AI180252	–1.27
66	Upk3a_predicted	uroplakin 3A (predicted)	315190	–1.52
67	RGD:1303270	proline-rich polypeptide 3	361788	–1.58
68	EST		BE116890	–1.64
69	Rasd2	RASD family, member 2	171099	–1.34
70	Bmpr1a	bone morphogenetic protein receptor, type 1A	81507	–1.37
71	EST		BF388585	–1.46
72	Hspa1a	heat shock 70-kDa protein 1A	24472	–1.6
73	EST		AI406912	–1.64
74	EST		BE104676	–1.38

More detailed list of genes whose expression was altered by NF-kappaB inhibition already after 6 h compared to untreated samples or samples treated with the inactive NF-kappaB inhibitor control and their corresponding 'fold change' values obtained by dChip analysis. Numbers 1–36 represent up-regulation of gene expression; numbers 37–74 represent down-regulation of gene expression. EST = Expressed sequence Taq.

3.4. Inhibition of PI3-K Reduces Caspase-3 Activation in OC Explants Exposed to an NF-kappaB Inhibitor

Activation of caspases (cysteine-aspartatic acid proteases) is an early event in programmed cell death. Caspases initiate cellular breakdown by degrading specific proteins. Activation of caspase-3 plays a key role in the apoptotic process, and once it has been activated, the program for cell death is irreversibly activated. In a recent report we showed that caspase-3 activity increases in the OC following inhibition of NF-kappaB activity [Nagy et al., 2005], suggesting that HC death following NF-kappaB inhibition occurs by an apoptosis-directed pathway. Caspase activity assays utilizing Ac-DEVD-pNA caspase-3 substrate (Alexis Biochemicals) indicated that inhibition of PI3-K significantly ($p = 0.0378$) reduced caspase-3 activity in OC explants exposed to the NF-kappaB inhibitor (fig. 6). As a negative control the baseline buffer and as a positive control an active human recombinant caspase-3 (Alexis Biochemicals) were used (data not shown).

4. Discussion

Inhibition of NF-kappaB activity in OC explants of p5 Sprague-Dawley rats resulted in up-regulation of 12 genes, among them the gene coding for PI3-Kr1, and down-regulation of 2 genes. Moreover, using cell culture experiments we show that the inhibition of the PI3-K signaling pathway, using a specific inhibitor, reduced caspase-3 activation in OC explants exposed to a specific NF-kappaB inhibitor. Moreover, we found with immunofluorescence PI3-Kr1 exclusively in HCs and not in supporting cells. These data provide evidence for involvement of the PI3-K signaling pathway in NF-kappaB-dependent HC death.

The NF-kappaB family of transcription factors are key regulators of many biological processes such as immunity, cell survival and apoptosis [Karin and Greten, 2005]. However, their function in the inner ear is only partially understood. NF-kappaB expression has been found in

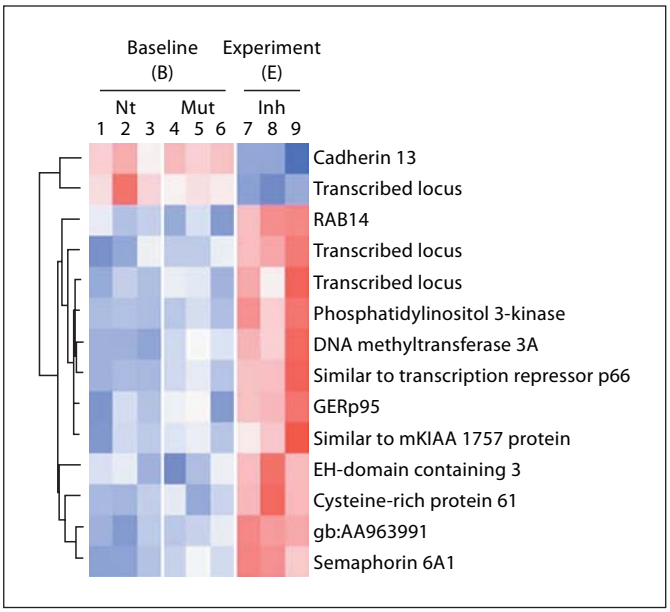

Fig. 3. Triplicate microarray data. Differentially expressed genes. Replicate assays from the same experimental condition (lanes 1, 2, and 3 represent untreated controls, lanes 4, 5, and 6 represent 6-hour treatment with the inactive NF-kappaB inhibitor control, whereas lanes 7, 8, and 9 represent 6-hour treatment with the NF-kappaB inhibitor) were pooled using a weighted averaging method and comparative analysis was performed using dChip software. After filtering, 14 genes depicted were identified as being reliably differentially expressed between the different groups (format is the same as in fig. 1).

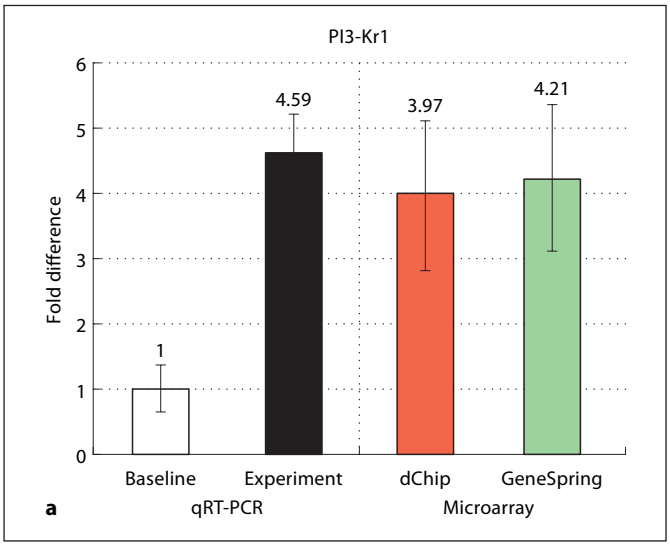

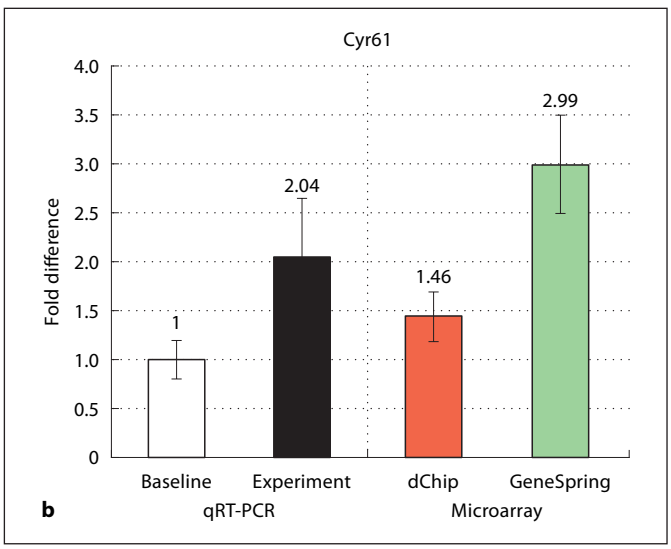

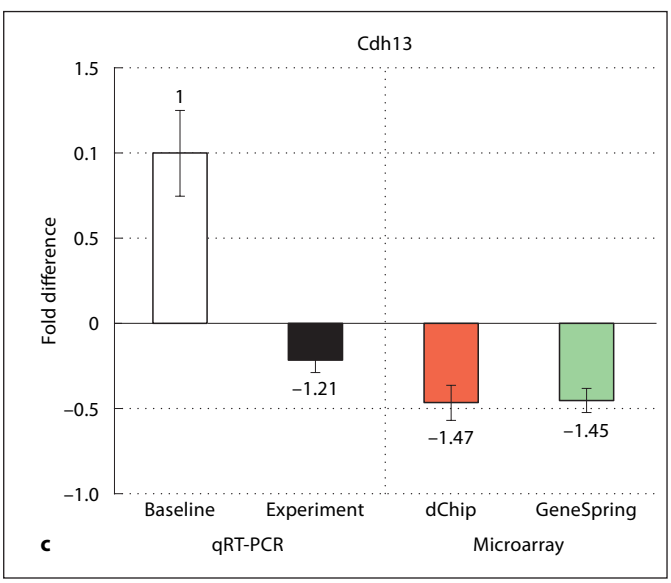

Fig. 4. Quantification of RT real-time PCR signals of PI3-Kr1 (**a**), Cdh13 (**c**) and Cyr61 (**b**) in untreated (control) and NF-kappaB-treated samples. Relative quantification of RT real-time PCR signals using the comparative C_t method is shown. Gusb serves as active endogenous control to which target mRNA was normalized; average values were calculated based on results from three independent experiments. Standard deviation is given by error bars. Expression values from dChip and GeneSpring are included for comparison.

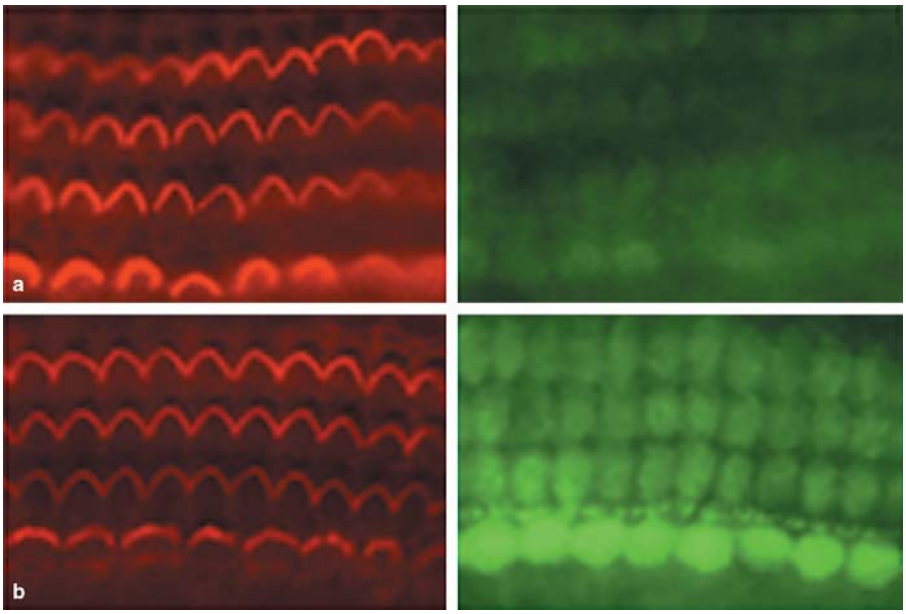

Fig. 5. Immunofluorescence showing PI3-Kr1 in inner and outer HCs before (**a**) and after (**b**) treatment for 6 h with a NF-kappaB inhibitor; the right side shows immunostaining for PI3-Kr1, the left side shows the corresponding phalloidin staining.

Table 2. Triplicate microarray data

NCBI locus	Gene name	Fold change dChip	Fold change GeneSpring
BI282750	cadherin-13	–1.47 ± 0.12	–1.45 ± 0.21
BF400182	transcribed locus	–1.82 ± 0.08	–1.64 ± 0.13
AA923974	RAB14	+1.39 ± 0.14	+1.43 ± 0.18
AI102401	transcribed locus	+1.52 ± 0.31	+1.46 ± 0.37
BM391695	transcribed locus	+1.49 ± 0.09	+1.41 ± 0.15
D64048	phosphatidylinositol 3-kinase	+3.97 ± 0.42	+4.21 ± 0.51
AI029751	DNA methyltransferase 3A	+1.60 ± 0.34	+1.53 ± 0.39
BE109744	similar to transcription repressor p66	+2.19 ± 0.32	+1.92 ± 0.42
BF281131	GERp95	+1.77 ± 0.43	+1.46 ± 0.52
AW526768	similar to mKIAA 1757 protein	+2.17 ± 0.49	+1.13 ± 0.50
AA957585	EH-domain containing 3	+1.37 ± 0.17	+1.67 ± 0.23
NM_031327	cysteine-rich protein 61	+1.46 ± 0.27	+2.99 ± 0.46
AA963991	Gb:AA963991	+1.46 ± 0.15	+1.39 ± 0.19
BM387083	semaphorin 6A 1	+1.61 ± 0.25	+1.46 ± 0.28

Genes of interest whose expression reliably differs in NF-kappaB inhibitor-treated versus control arrays. Fold changes in expression levels with respect to the untreated control samples (± standard deviation between triplicate experiments) are given.

the murine cisplatin-treated cochlea, mostly in the stria vascularis and the spiral ligament [Watanabe et al., 2002]. Recently, it has been reported that NF-kappaB has a protective role in kanamycin-induced HC death in adult mice [Jiang et al., 2005]. In addition, we have shown that NF-kappaB is found in the immature OC in a constitutive active form and that inhibition of its activity results in massive HC degeneration [Nagy et al., 2005]. In order to investigate downstream events that contribute to apoptotic HC death in response to NF-kappaB inhibition in the immature cochlea, we initiated this study.

We primarily wanted to gain insight into early gene expression changes that occur in the OC after NF-kappaB inhibition, which ultimately lead to, but occur prior

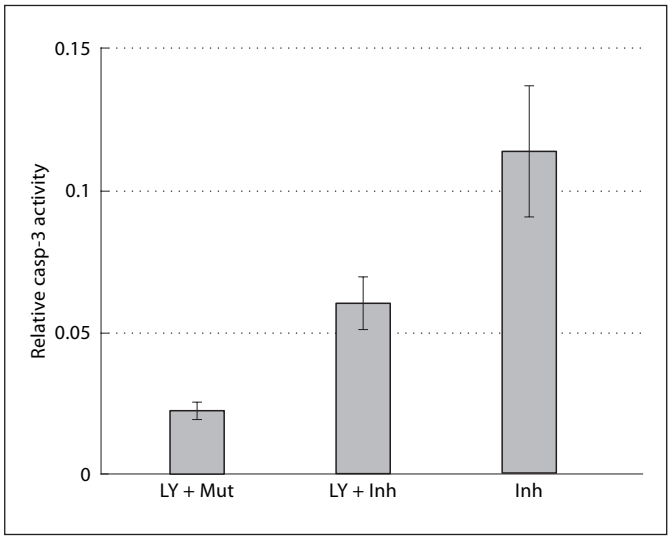

Fig. 6. Inhibition of phosphatidylinositol 3-kinase reduces caspase-3 activity in OC exposed to an NF-kappaB inhibitor. Caspase-3 activation assay; phosphatidylinositol 3-kinase inhibitor and control for NF-kappaB inhibitor (LY + Inh-Mut), phosphatidylinositol 3-kinase inhibitor and NF-kappaB inhibitor (LY + Inh), or NF-kappaB inhibitor (Inh). Baseline buffer and Ac-DEVD-pNA activity (as measured in sample not containing protein lysates) were subtracted from each sample. Data bars represent mean values obtained in three independent experiments, and error bars represent standard deviation.

to the actual death of HCs. Two genes, encoding for Cyr61 and PI3-Kr1, seemed to be most interesting because of the reports from the literature linking them to NF-kappaB [Beraud et al., 1999; Birkenkamp et al., 2004; Lin et al., 2004]. Even though there are no data in the literature concerning the role of Cyr61 in the ear, Lin et al. [2004] report that MCF-7 cell lines overexpressing Cyr61 had significantly increased NF-kappaB activity compared with control cells. Furthermore, the NF-kappaB pathway was evidently activated in Cyr61-overexpressing gastric cancer cells [Lin et al., 2005]. Reports by Reddy et al. [1997], Beraud et al. [1999] and Birkenkamp et al. [2004] made a connection also between PI3-K and NF-kappaB. Real-time PCR confirmed down-regulation of Cdh13 in OC explants after NF-kappaB inhibition. The significance of the changes in Cdh13 and Cyr61 expression in OC explants after NF-kappB inhibition has to be elucidated in future studies. In this study we focus on the PI3-K signaling pathway.

PI3-K generates phosphorylated phosphoinositides that serve as crucial second messengers for a wide range of biological functions such a cell survival and differentiation. The role of the PI3-K signaling pathway in the inner ear is poorly understood. It has been demonstrated that this pathway plays a role for S-phase entry of the vestibular epithelia of both avian and mammalian species [Witte et al., 2001].

Recent studies in other cell types indicate a complex regulation of PI3-K activity involving a delicate balance between the regulatory subunits and functional PI3-K heterodimers consisting of regulatory and catalytic subunits [Fruman et al., 1998; Hallmann et al., 2003; Katso et al., 2001; Virkamaki et al., 1999]. In this study we found PI3-Kr1 up-regulated after NF-kappaB inhibition in OC explants. Moreover we found weak immunoreactivity of PI3-Kr1 in control explants, and strong immunoreactivity in OC explants exposed to the NF-kappaB inhibitor. In both cases PI3-Kr1 was detected in hair cells and not in supporting cells of the OC. This is very much in agreement with findings by Beraud et al. [1999]. They have reported that PI3-Kr1 specifically associates with tyrosine-phosphorylated IkappaB-alpha after stimulation of T cells with pervanadate. This suggests that by sequestering IkappaB-alpha, PI3-Kr1 is involved in an alternative pathway of activating NF-kappaB. Therefore it is possible that by increasing the expression of PI3-Kr1 HCs are trying to reduce the impact of apoptosis caused by NF-kappaB inhibition. These findings suggest that up-regulation of the regulatory subunit of PI3-K upon NF-kappaB inhibition might work as a counterbalance to the process of apoptosis and help rescue the cells.

What about the role of PI3-K itself? Beraud et al. [1999], Birkenkamp et al. [2004] and Reddy et al. [1997] have found, under conditions when NF-kappaB was activated, that inhibition of PI3-K resulted in reduction of NF-kappaB activity. In this study, however, inhibition of PI3-K activity with LY294002, a compound that affects the ATP binding site of the enzyme [Vlahos et al., 1994], reduced caspase-3 activity in OC explants exposed to a NF-kappaB inhibitor. It should be noted that inhibition of PI3-K under normal culturing conditions did not result in morphological changes of HCs. This suggests that, under conditions when NF-kappaB is inhibited, inhibition of PI3-K helps alleviate the effect of apoptosis. Why does inhibition of PI3-K not increase the effect of apoptosis, as would be expected from the reports above? We suggest the following explanation: under conditions of NF-kappaB inhibition, the expression of the regulatory subunit of PI3-K in HCs is increased and it becomes in excess over the PI3-K heterodimers. It has been proposed that excess monomeric regulatory subunit competes with

functional PI3-K heterodimers [Hallmann et al., 2003]. Inhibition of the catalytic site of the enzyme by a specific inhibitor might contribute to shifting the balance to the side of the regulatory subunit, which, by sequestering the IkappaB-alpha, could help diminish the effect of inhibition of NF-kappaB and subsequently reduce apoptosis. However, additional experiments are required to confirm this hypothesis.

This study links the PI3-K pathway to NF-kappaB-dependent HC death in the immature mammalian cochlea. However, one should be aware of several limitations of the methods used. First of all, since mature HCs cannot be maintained in vitro, we have used immature HCs for this study. Even though immature cochlea is an established model for cellular and molecular studies concerning various aspects of inner ear biology such as ototoxicity [Pirvola et al., 2000], immature HCs can react differentially than adult HCs to inhibition of intracellular signaling pathways. Therefore our data are limited to the immature mammalian cochlea. What might be the role of NF-kappaB in the mature cochlea? Recent studies indicate a role for NF-kappaB in the mature cochlea: a study conducted with adult mice demonstrated that the redox state of the cochlea stimulates NF-kappaB activation [Jiang et al., 2005]. In another study, adult mice lacking the NF-kappaB subunit p50 suffered from increased noise-induced hearing loss compared to their wild-type littermates [Lang et al., 2006]. It seems therefore that NF-kappaB plays an important role in the adult mammalian cochlea. However, although the microarray data were analyzed by two independent comparative analyses that gave overlapping results and the data were confirmed by RT real-time PCR and by using highly specific signal transduction pathway inhibitors, one must be aware that the use of microarray technology is not well established for the analysis of gene expression in the inner ear. Due to the fact that no inner ear array (no high-quality inner ear arrays commercially available at this time) has been used in this study, it is possible that some genes specifically differentially expressed in the OC were missed. Additionally, we might have missed some genes because we applied very stringent filtering criteria for selecting the 14 differentially expressed genes in the replicate experiment. While such criteria contributed to the reliability of the data, they may have caused the loss of some genes. Another difficulty that arises when microarray technology is applied to analysis of gene expression in the inner ear, is how to discern differences in cell type-specific expression, as there are different cell types in the OC of the inner ear. Therefore our microarray data reflect the global gene expression pattern from all the cells of the OC and not only of HCs. However, in a previous study [Nagy et al., 2005], we have shown that NF-kappaB is localized in the nuclei of HCs in the OC, suggesting that the molecular mechanisms involved after NF-kappaB inhibition are also localized in HCs.

Taken together, this study suggests that the PI3-K pathway is involved in the NF-kappaB-dependent HC death in the immature mammalian cochlea. The involvement of other genes identified by the microarray experiment described herein was not confirmed. Their role is currently unknown and will be addressed in further studies.

Acknowledgments

We thank Dr. Marzanna Kuenzli, who performed the microarrays, and Dr. Ulrich Wagner (both from the Functional Genomics Center Zurich, ETH) for assistance with bioinformatics; Dr. Mathias Höchli (Electron Microscopy Unit, University of Zurich) for help with confocal imaging, and Verena Hoffmann (University Hospital Zurich) for technical assistance. This work was supported by the Swiss National Science Foundation Grant No. 320000-107553.

References

Beraud C, Henzel WJ, Baeuerle PA: Involvement of regulatory and catalytic subunits of phosphoinositide 3-kinase in NF-kappaB activation. Proc Natl Acad Sci USA 1999;96:429–434.

Birkenkamp KU, Geugien M, Schepers H, Westra J, Lemmink HH, Vellenga E: Constitutive NF-kappaB DNA-binding activity in AML is frequently mediated by a Ras/PI3-K/PKB-dependent pathway. Leukemia 2004;18:103–112.

Cheng L, Wing HW: Model-based analysis of oligonucleotide arrays: expression index computation and outlier detection. Proc Natl Acad Sci USA 2001;98:31–36.

D'Addario M, Ahmad A, Xu JW, Menezes J: Epstein-Barr virus envelope glycoprotein gp350 induces NF-kappaB activation and IL-1beta synthesis in human monocytes-macrophages involving PKC and PI3-K. FASEB J 1999;13:2203–2213.

Fruman DA, Meyers RE, Cantley LC: Phosphoinositide kinases. Annu Rev Biochem 1998;67:481–507.

Hallmann D, Trumper K, Trusheim H, Ueki K, Kahn CR, Cantley LC, Fruman DA, Horsch D: Altered signaling and cell cycle regulation in embryonal stem cells with a disruption of the gene for phosphoinositide 3-kinase regulatory subunit p85alpha. J Biol Chem 2003;278:5099–5108.

Huang T, Cheng AG, Stupak H, Liu W, Kim A, Staecker H, Lefebvre PP, Malgrange B, Kopke R, Moonen G, Van De Water TR: Oxidative stress-induced apoptosis of cochlear sensory cells: otoprotective strategies. Int J Dev Neurosci 2000;18:259–270.

Hubbell E, Liu WM, Mei R: Robust estimators for expression analysis. Bioinformatics 2002; 18:1585–1592.

Jiang H, Sha SH, Schacht J: NF-kappaB pathway protects cochlear hair cells from aminoglycoside-induced ototoxicity. J Neurosci Res 2005;79:644–651.

Johnsson LG, Hawkins JE Jr, Kingsley TC, Black FO, Matz GJ: Aminoglycoside-induced cochlear pathology in man. Acta Otolaryngol Suppl 1981;383:1–19.

Kaltschmidt C, Kaltschmidt B, Neumann H, Wekerle H, Baeuerle PA: Constitutive NF-kappa B activity in neurons. Mol Cell Biol 1994;14:3981–3992.

Karin M, Greten FR: NF-kappaB: linking inflammation and immunity to cancer development and progression. Nat Rev Immunol 2005;5:749–759.

Katso R, Okkenhaug K, Ahmadi K, White S, Timms J, Waterfield MD: Cellular function of phosphoinositide 3-kinases: implications for development, homeostasis, and cancer. Annu Rev Cell Dev Biol 2001;17:615–675.

Krishnamoorthy RR, Crawford MJ, Chaturvedi MM, Jain SK, Aggarwal BB, Al-Ubaidi MR, Agarwal N: Photo-oxidative stress down-modulates the activity of nuclear factor-kappaB via involvement of caspase-1, leading to apoptosis of photoreceptor cells. J Biol Chem 1999;274:3734–3743.

Lang H, Schulte BA, Zhou D, Smythe N, Spicer SS, Schmiedt RA: Nuclear factor kappaB deficiency is associated with auditory nerve degeneration and increased noise-induced hearing loss. J Neurosci 2006;26:3541–3550.

Lin MT, Chang CC, Chen ST, Chang HL, Su JL, Chau YP, Kuo ML: Cyr61 expression confers resistance to apoptosis in breast cancer MCF-7 cells by a mechanism of NF-kappaB-dependent XIAP up-regulation. J Biol Chem 2004;279:24015–2423.

Lin MT, Zuon CY, Chang CC, Chen ST, Chen CP, Lin BR, Wang MY, Jeng YM, Chang KJ, Lee PH, Chen WJ, Kuo ML: Cyr61 induces gastric cancer cell motility/invasion via activation of the integrin/nuclear factor-kB/cyclooxygenase-2 signaling pathway. Clin Cancer Res 2005;11:5809–5820.

Liu WM, Mei R, Di X, Ryder TB, Hubbell E, Dee S, Webster TA, Harrington CA, Ho MH, Baid J, Smeekens SP: Analysis of high density expression microarrays with signed-rank call algorithms. Bioinformatics 2002; 18:1593–1599.

Nadol Jr JB: Hearing loss. N Engl J Med 1993; 329:1092–1102.

Nagy I, Monge A, Albinger-Hegyi A, Schmid S, Bodmer D: NF-κB is required for survival of immature auditory hair cells in vitro. J Assoc Res Otolaryngol 2005;6:260–268.

Pirvola U, Xing-Qun L, Virkkala J, Saarma M, Murakata C, Camoratto AM, Walton KM, Ylikoski J: Rescue of hearing, auditory hair cells, and neurons by CEP-1347/KT7515, an inhibitor of c-Jun N-terminal kinase activation. J Neurosci 2000;20:43–50.

Reddy SA, Huang JH, Liao WS: Phosphatidylinositol 3-kinase in interleukin 1 signaling: Physical interaction with the interleukin 1 receptor and requirement in NFkappaB and AP-1 activation. J Biol Chem 1997;272: 29167–29173.

Sobkowicz HM, Loftus JM, Slapnick SM: Tissue culture of the organ of Corti. Acta Otolaryngol Suppl 1993;502:3–36.

Virkamaki A, Ueki K, Kahn CR: Protein-protein interaction in insulin signaling and the molecular mechanisms of insulin resistance. J Clin Invest 1999;103:931–943.

Vlahos CJ, Matter WF, Hui KY, Brown RF: A specific inhibitor of phosphatidylinositol 3-kinase, 2-(4-morpholinyl)-8-phenyl-4H-1-benzopyran-4-one (LY294002). J Biol Chem 1994;269:5241–5248.

Watanabe K, Inai S, Jinnouchi K, Bada S, Hess A, Michel O, Yagi T: Nuclear-factor kappa B (NF-kappa B)-inducible nitric oxide synthase (iNOS/NOS II) pathway damages the stria vascularis in cisplatin-treated mice. Anticancer Res 2002;22:4081–4085.

Witte MC, Montcouquiol M, Corwin JT: Regeneration in avian hair cell epithelia: identification of intracellular signals required for S-phase entry. Eur J Neurosci 2001;14: 829–838.

Yorgason JG, Fayad JN, Kalinec F: Understanding drug ototoxicity: molecular insights for prevention and clinical management. Expert Opin Drug Saf 2006;5:383–399.